

**Structural and biochemical consequences of disease-causing mutations in the ankyrin
repeat domain of the human TRPV4 channel**

Hitoshi Inada, Erik Procko, Marcos Sotomayor, and Rachelle Gaudet

Supporting Information

Table S1. TRPV-ARD structures used in this study

Protein	Species	Structure (# mol/a.u.)	ATP binding	References
TRPV1	Rat	2PNN (1), 2NYJ (1)	+	Lishko <i>et al.</i> , 2007 (ATP-bound forms)
TRPV2	Rat	2ETA (2), 2ETB (1), 2ETC (2)	–	Jin <i>et al.</i> , 2006
	Human	2F37 (2)		McCleverty <i>et al.</i> , 2006
TRPV4	Human	Form I 4DX1 (2) without ATP	+	This study
		Form II 4DX2 (2) with 5 mM ATP		
	Chicken	3JXI (4), 3JXI (2)	+	Landouré <i>et al.</i> , 2010 (ATP-free forms)
TRPV6	Mouse	2RFA (1)	–	Phelps <i>et al.</i> , 2008

Table S2. Structural similarity between TRPV4-ARD and other TRPV-ARDs

TRPV	TRPV1	TRPV2			TRPV6	TRPV4	
Species	Rat	Rat		Human	Mouse	Chicken	
PDB	2PNN	2ETB	2ETC ^a	2F37 ^a	2RFA	3JXI ^a	3JXJ ^a
RMSD ^b							
Finger 2 ^c	1.596 / 0.279	1.527 / 0.245	1.251 / 1.081	1.577 / 0.227	1.538 / 0.259	0.183 / 1.599	0.213 / 1.617
Finger 3 ^d	4.588 / 1.762	5.168 / 2.444	3.652 / 3.941	5.266 / 1.949	5.135 / 1.972	3.587 / 4.732	2.934 / 4.393
Core ^e	1.593 / 1.653	1.378 / 1.457	1.451 / 1.573	1.463 / 1.541	1.865 / 1.736	0.691 / 0.737	0.637 / 0.676

^a Only the chains with complete loops were used in the analysis. ^b RMSD to human TRPV4-ARD (ATP-free, form I / ATP-bound, form II). ^c Residues 229-240 in hTRPV4. ^d Residues 261-287 in hTRPV4. ^e Residues 152-176, 194-228, 241-260, 288-307, 324-356, 373-394 in hTRPV4.

Table S3. Molecular dynamics simulations of rat TRPV1-ARD

Label	t_{sim} (ns)	Type [†]	Ensemble	SMD atoms	Speed (nm/ns)
	1.1 [‡]	<i>EQ</i>	NpT	-	-
TRPV1-ARD- ATP	1.6	<i>SMD</i>	NVE	L111-C α /H358-C α	20
	8.3	<i>SMD</i>	NpT	L111-C α /H358-C α	2
	1.1 [‡]	<i>EQ</i>	NpT	-	-
TRPV1-ARD-Apo	1.6	<i>SMD</i>	NVE	L111-C α /H358-C α	20
	8.3	<i>SMD</i>	NpT	L111-C α /H358-C α	2

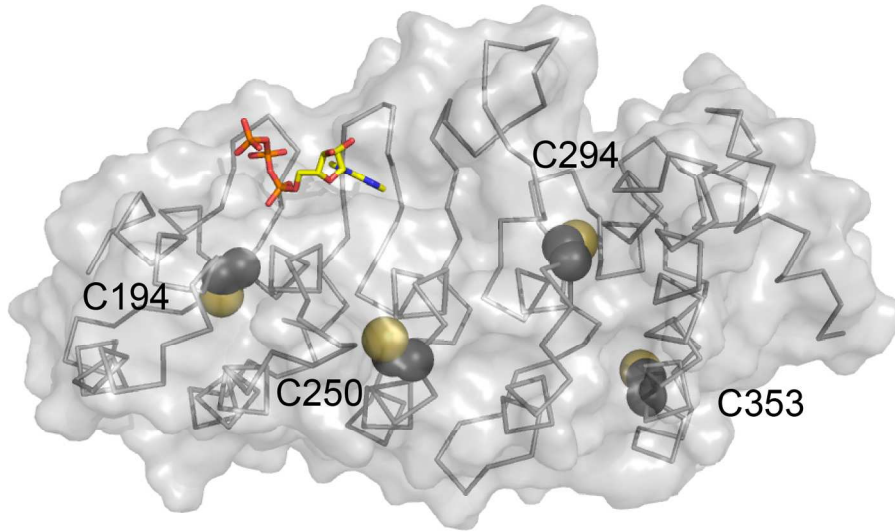
[†] EQ denotes equilibrium simulations and SMD denotes constant velocity steered molecular dynamics.

[‡] These simulations consisted of 1,000 steps of minimization, 100 ps of dynamics with the backbone of the protein restrained ($k = 1$ kcal/mol/Å²), and the remaining time as free dynamics in the NpT ensemble (Langevin damping set to 1 ps⁻¹).

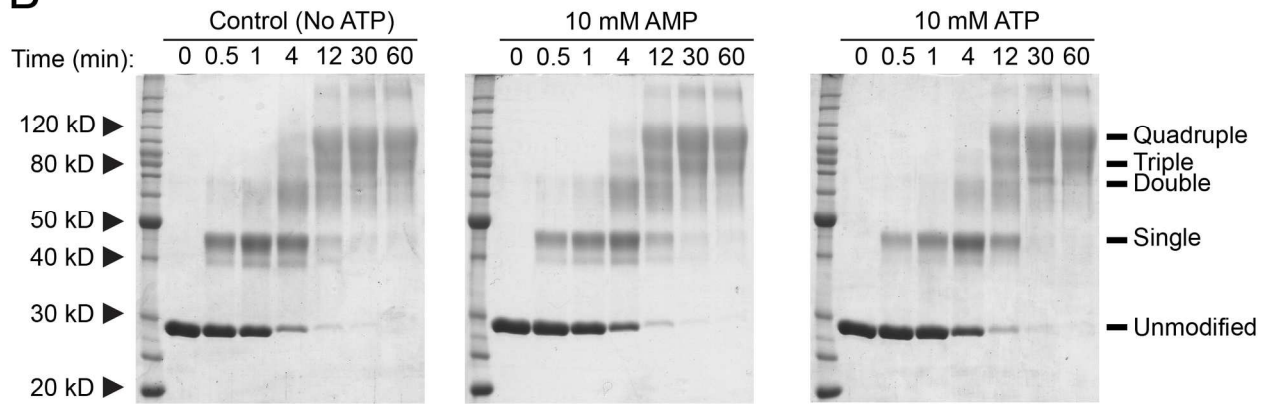
Table S4. T_m of wildtype and mutant TRPV4-ARD proteins

Protein	N	Mean		Std Dev		p-Value	
		T _m	±	(°C)			
WT	8	37.93	±	0.08		1	
E183K	3	33.78	±	0.06		<.0001	*
K197R	3	35.3	±	0.1		<.0001	*
L199F	3	32.9	±	0.1		<.0001	*
R232C	3	38.1	±	0.1		0.8415	
R269C	3	38.6	±	0.2		<.0001	*
R269H	3	36.8	±	0.3		<.0001	*
E278K	3	37.3	±	0.2		<.0001	*
R315W	3	36.2	±	0.2		<.0001	*
R316C	3	34.7	±	0.3		<.0001	*
I331F	3	35.5	±	0.2		<.0001	*
I331T	3	37.97	±	0.07		1	
D333G	3	36.4	±	0.2		<.0001	*
V342F	3	35.4	±	0.3		<.0001	*

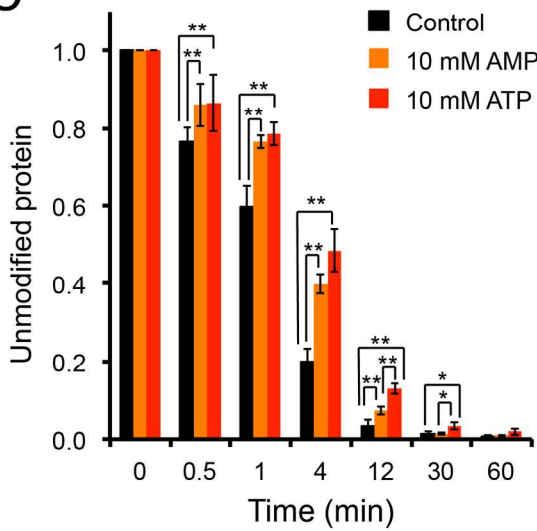
A



B



C



D

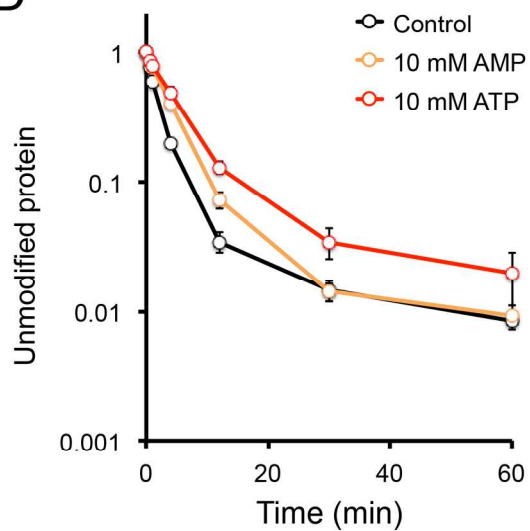


Figure S1. ATP binding effect on protein folding/flexibility in hTRPV4-ARD. A, hTRPV4-ARD contains four cysteines (Cys194, Cys250, Cys294, and Cys353; spheres). Bound ATP is shown as yellow sticks. Cys194 corresponds to Cys157 in TRPV1, which is required for activation by chemical modification with allicin, a garlic extract compound.¹ B, Time course for modification of hTRPV4-ARD cysteines by PEG-maleimide (mPEG). Reactions containing hTRPV4-ARD (8.5 μ M) in 150 mM NaCl, 20 mM Tris (pH 7.0), 0.5 mM mPEG-5 kDa (Creative PEGWorks) and 10 mM nucleotide as indicated, were incubated at room temperature, stopped by addition of DTT to 110 mM, and analyzed by Coomassie-stained 12% SDS-PAGE. hTRPV4-ARD modification at cysteine residues resulted in electrophoretic mobility shifts on a Coomassie-stained SDS-gel. Unmodified protein is reduced and modified proteins (single, double, triple, and quadruple) are increased in a time-dependent manner. Shown is a representative Coomassie-stained gel from one of three experiments. The statistical significance of the change in unmodified protein with respect to time point 0 was determined by a multiple comparison test using Tukey-Kramer method, with $p < 0.05$ and $p < 0.01$ indicated by * and **, respectively. C, Amount of unmodified protein in (B) is quantified as the mean \pm standard deviation. D, Same data as in (C) with vertical axis in log scale.

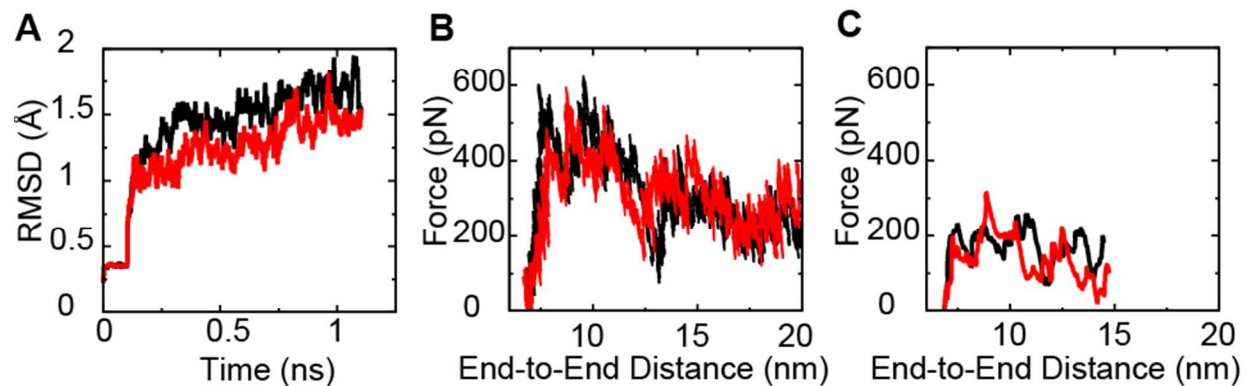


Figure S2. Stability of TRPV1-ARD in equilibrium and SMD simulations. A, Root mean square deviation (RMSD) is shown versus time during equilibrium simulations in the presence (red) and absence (black) of ATP. B and C, Force required to stretch and unfold TRPV1-ARD is shown as a function of the protein's end-to-end distance for simulations performed at 20 (B) and 2 nm/ns (C) with (red) and without (black) bound ATP.

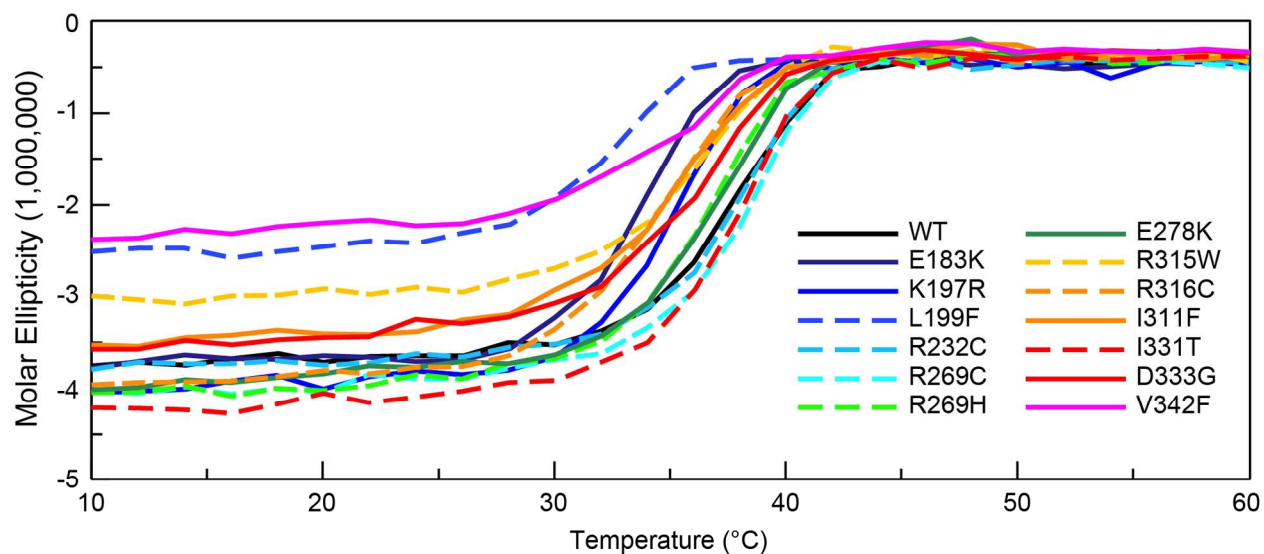


Figure S3. The thermal stability of wildtype and mutant TRPV4-ARD proteins. The molar ellipticity at $\lambda = 222$ nm was measured as the protein solutions were heated by 1 °C/min.

Supplementary References

1. Salazar, H., Llorente, I., Jara-Oseguera, A., Garcia-Villegas, R., Munari, M., Gordon, S. E., Islas, L. D., and Rosenbaum, T. (2008) A single N-terminal cysteine in TRPV1 determines activation by pungent compounds from onion and garlic, *Nat Neurosci* 11, 255-261.